

Surface reactivity of Pd nanoparticles supported on polycrystalline substrates as compared to thin film model catalysts: infrared study of CH₃OH adsorption

Serena Bertarione,^{a,b} Domenica Scarano,^{a,b} Adriano Zecchina,^{a,b,*} Viktor Johánek,^c Jens Hoffmann,^c Svetlana Schauer mann,^c Jörg Libuda,^c Günther Rupprechter,^c and Hans-Joachim Freund^c

^a Dipartimento di Chimica Inorganica, Chimica Fisica e Chimica dei Materiali, Università di Torino, via P. Giuria 7, 10125 Torino, Italy

^b Consorzio INSTM, via Benedetto Varchi n. 59, 50132 Firenze, Italy

^c Fritz-Haber-Institut der Max-Planck-Gesellschaft, Faradayweg 4-6, 14195 Berlin, Germany

Received 25 September 2003; revised 8 January 2004; accepted 8 January 2004

Abstract

A detailed comparative study of CH₃OH adsorption on two categories of supported Palladium nanoparticles is reported: (1) MgO and γ -Al₂O₃-supported Pd metal catalysts prepared by impregnation techniques and characterized by different degrees of regularity and perfection and (2) single-crystal-based Pd/Al₂O₃ model catalysts prepared under ultrahigh vacuum (UHV) conditions. A detailed structural characterization of the supported Pd nanoparticles allows the assignment of vibrational frequencies of CH₃OH and its decomposition products to well-defined types of sites on these systems. The decomposition of methanol on both types of catalysts is compared as an example for a reactivity study. On the model catalyst, infrared reflection–absorption spectroscopy (IRAS) experiments shed light on the role of two decomposition pathways, dehydrogenation and C–O bond scission. The effect of carbon contamination in the vicinity of edge and defect sites is explored. For the Pd/MgO systems studied by transmission FTIR, a mechanism for the methanol decomposition/synthesis is proposed, which involves the simultaneous formation of carbonyl species on Pd particles (at room temperature) and methoxy on the MgO matrix. The MgO matrix is basic and hence the surface OH groups can react with CO species initially formed on Pd particles and spilled onto the matrix. This reaction channel results in the formation of intermediates with a formate-type structure, which can be easily detected by IR spectroscopy. The superior activity of Pd/MgO in the decomposition/synthesis of methanol is explained on the basis of a cooperative effect between the Pd particles and the basic matrix.

© 2004 Elsevier Inc. All rights reserved.

Keywords: Molecular beams; Infrared spectroscopy; IRAS; FTIR; Microscopy; TEM; Aluminum oxide-supported model catalysts; Polycrystalline magnesium oxide-supported metal; Palladium; Methanol

1. Introduction

It is known that the reactivity of heterogeneous catalysts depends not only on the type of materials involved but also on the morphology and size of the metal particles dispersed on a support, on the presence of promoters and poisons, and on the type of the support [1]. This implies that the catalytic activity of nanoparticles is critically controlled by their microscopic structure, by the presence of

coadsorbed species, and by the metal–support interactions. In many cases it is assumed that the particular reactivity of such surfaces arises from the simultaneous presence of different active sites [2,3].

Effects of the crystallite size and the degree of metal dispersion have been extensively studied in connection with the catalytic activity and selectivity of supported transition-metal catalysts for many reactions [4–8]. For this purpose it is important to verify whether such effects depend on the nature of supporting materials as well. For highly dispersed metal catalysts, it is known that the effect of metal support interaction (MSI) and metal crystallite size on the activity and reducibility are closely related. In particular,

* Corresponding author.

E-mail address: adriano.zecchina@unito.it (A. Zecchina).

an enhanced metal–support interaction, due to electron-transfer effects, is observed with increasing degrees of metal dispersion. This phenomenon can cause a depression of chemisorption uptake and a suppression of catalytic activity in the case of oxide supports, which are reducible at elevated temperatures [9]. Moreover, it is well established that different preparation methods and precursors considerably affect the dispersion and, therefore, the catalytic activity [9–11].

Recent works, concerning noble metal catalysts, have found supported Pd systems to be active for important processes such as synthesis or the partial and total oxidation of methanol at relatively low temperatures [2,12–17]. Interestingly, these catalysts show pronounced support, size, and promoter effects [18–27]. Despite the large impact of these effects, there is hardly any detailed understanding of their molecular origins [28,29]. This lack of knowledge is related to serious experimental problems in studies on real catalysts and to the enormous complexity of their surfaces. To elucidate the size and promoters effects, a number of studies have been performed on the reactivity of methanol under UHV conditions, both on single Pd crystals [30–38] and on Pd film [39]. The mechanistic issues regarding the decomposition on transition-metal surfaces have been reviewed by Mavrikakis and Barteau [40] recently.

In contrast to the metal single crystals, supported model catalysts allow us to design surfaces that resemble specific features of real catalysts [41–45], but avoid the full complexity of these materials. Here, we combine this approach with the use of molecular beam techniques and in situ infrared reflection absorption spectroscopy (IRAS), yielding detailed kinetic data under well-controlled conditions [46–50].

Specifically, we investigate the adsorption and decomposition of CH₃OH on a Pd model catalyst, which is based on an ordered alumina model support, obtained by oxidation of the NiAl(110) face [46,47]. The results are compared with those obtained on Pd particles supported on γ -Al₂O₃, on pure MgO and on Cl-doped MgO high surface area systems.

The IR data obtained for the Pd/Al₂O₃ system are not reported in detail, because they are not substantially different from those obtained on a Cl-doped Pd/MgO system (which on the contrary is discussed in detail). The choice of MgO as support is also motivated by its structural simplicity and the observations reported in the literature [27] that the basic metal oxides as cocatalysts and Pd/MgO systems have superior activity in methanol synthesis. As this fact seems to imply that the surface basicity can be a promoting factor of the reactivity of Pd particles [27], we have also studied the Pd/MgO(Cl) system, where the surface basicity is strongly depressed by the presence of Cl. In agreement with the hypothesis that the surface basicity is playing a role, the Pd/Al₂O₃ system does not show peculiar properties in methanol synthesis.

The final aim of the comparison of the results obtained on Pd particles on ordered films and on dispersed oxides is to highlight the contribution to the catalytic activity of the

particle dimension and morphology, together the promoting effect of the support.

In particular in this paper the following topics will be discussed in detail:

1. the plausible pathways for the methanol decomposition/synthesis on Pd model systems;
2. the plausible pathways for the methanol decomposition/synthesis processes on polycrystalline MgO-supported Pd and the role of the basicity of MgO support in this reaction.

2. Experimental

As described in detail in Ref. [51], MgO-supported palladium catalysts (2.5, 5, and 10 wt% Pd) were prepared by impregnation of Mg(OH)₂ with solutions of either PdCl₂ or [Pd(NH₃)₄](NO₃)₂ and then dried at 403 K overnight, the former being calcined in air at 773 K for 4 h. All the samples were treated in vacuum in the IR quartz cell at 623 K and then reduced at temperatures ranging from 723 to 773 K. In this paper Pd/MgO(Cl) (2.5 wt% Pd) and Pd/MgO (10 wt% Pd) are compared, being the same samples accurately characterized in a previous contribution [51]. Both the Pd/MgO(Cl) and Pd/MgO outgassed samples were dosed with CH₃OH and heated in a CH₃OH atmosphere. The Pd/MgO system obtained from [Pd(NH₃)₄](NO₃)₂ impregnation was also heated in a CO/H₂ mixture (1/2). The FTIR spectra were recorded at 300 K in situ at 2 cm⁻¹ resolution, using a Bruker IFS 28 spectrometer, equipped with a cryogenic MCT detector. The morphological and structural characterization has been carried out by transmission electron microscopy (TEM, Jeol JEM 200 EX and Philips CM 200 FEG operated at 200 kV).

IRAS experiments on the single-crystal-based model catalyst have been performed in a UHV molecular beam/IRAS apparatus, which combines several independent beam sources, gas-phase detection, and in situ time-resolved IRAS. Briefly, the model catalysts are based on an ordered Al₂O₃ film grown on NiAl(110) [46,47] on which Pd is deposited under UHV (ultrahigh vacuum) conditions. Via choosing the appropriate preparation parameters, structure, size, and density of the Pd aggregates are controlled [43, and references therein]. More details concerning the preparation conditions and structure of the Pd particles can be found elsewhere [51,52]. Briefly, the Pd particles have an average size of approximately 6 nm and contain about 3000 Pd atoms each. They exhibit the morphology of well-ordered crystallites, growing in (111) orientation, and expose preferentially (111) facets as well as a small fraction of (100) facets. Methanol was dosed from a supersonic beam of CH₃OH (Merck, > 99.8%) in Ar (Messer Griesheim, 99.998%) as a carrier gas (CH₃OH flux: 6 × 10¹³ molecules cm⁻² s⁻¹).

3. Results and discussion

3.1. Morphological characterization of polycrystalline MgO-supported Pd crystallites

Both MgO-supported palladium catalysts were examined by transmission electron microscopy.

Fig. 1a shows the Pd/MgO(Cl) catalysts and by analyzing ~ 100 particles a mean particle diameter of 15 ± 3.5 nm was determined. In many cases the Pd particles have polygonal outlines with straight edges and rounded corners, suggesting well-developed facets. Similar particles can be found in the Pd/MgO catalyst (Fig. 1b), which in addition contains smaller Pd particles, leading to a mean size of about 11 ± 4.5 nm. The Pd particles of this catalyst often have rather irregular outlines, in particular those below 10 nm size. Fig. 1b also suggests that on the Pd/MgO system the total Pd loading and the specific surface area of Pd particles were higher than on Pd/MgO(Cl), which explains the intensity difference of the IR spectra of CO adsorbed on the two samples, as widely discussed in Ref. [51].

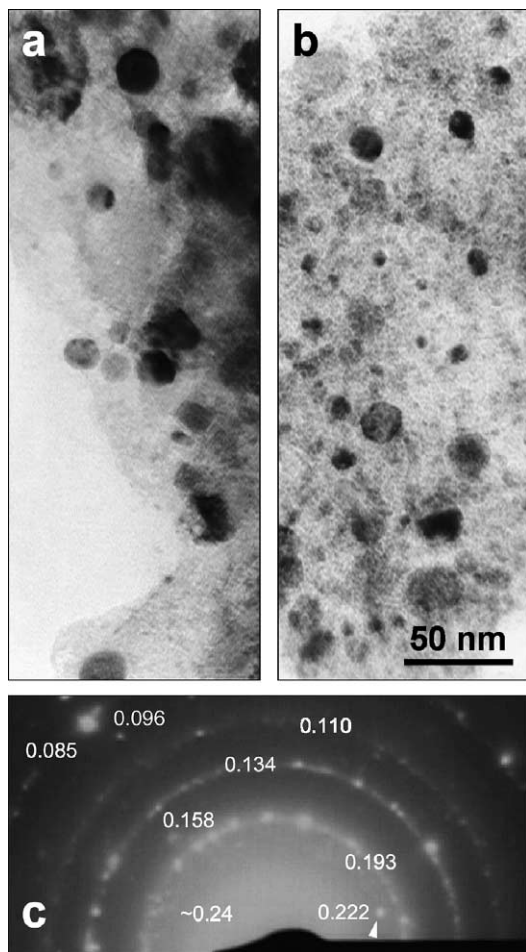


Fig. 1. Transmission electron micrographs of Pd particles on polycrystalline MgO surfaces (2.5 wt% Pd): (a) Pd/MgO(Cl); (b) Pd/MgO; (c) shows an electron diffraction pattern from Pd/MgO(Cl); see text.

The crystallinity of the Pd particles in both catalysts was confirmed by transmission electron diffraction (TED). As an example, Fig. 1c shows a diffraction pattern of the Pd/MgO(Cl) catalyst (because a diffraction pattern is centrosymmetric, only half is shown). It displays a typical pattern of randomly oriented particles producing “rings” that are often broken up into individual reflections. Since only a limited number of catalyst grains contributes to TED, a perfect ring pattern (as one would expect from powder X-ray diffraction) is not obtained. The experimentally observed interplanar distances (accuracy of about ± 0.005 nm) are also indicated in Fig. 1c. The reflections at 0.222, 0.193, 0.134, and 0.110 nm can be attributed to Pd(111), (200), (220), and (222), respectively. It should be noted that their relative intensity may vary with sample position since only a limited number of catalyst grains contributes to the pattern. Reflections around 0.24 nm (which are nearly obscured by the undiffracted beam) and 0.158 nm are due to the MgO support ((111) and (220)). Weak spots/rings at 0.096 and 0.085 nm are the higher order (400) and (420) reflections of Pd. TED of the other Pd/MgO catalyst showed similar patterns. For TEM and scanning tunneling microscopy (STM) images of Pd–Al₂O₃ model catalysts we refer to [43].

3.2. FTIR spectra of CH₃OH adsorbed on Pd/MgO(Cl) and Pd/MgO samples as compared with pure MgO

From FTIR spectra of CH₃OH, dosed on Pd/MgO(Cl) at 300 K and then heated in CH₃OH atmosphere at 473 K (Fig. 2), the following features can be seen:

1. Broad and intense bands in the $\nu \cong 3600\text{--}3200$ cm⁻¹ range together with an absorption at ~ 1043 cm⁻¹ are clearly observable after dosing CH₃OH at 300 K (2.66 kPa). These bands are easily removed by decreasing the pressure and, therefore, they are assigned to weakly adsorbed (hydrogen bonded) CH₃OH. It is noteworthy that these bands, together with the characteristic C–O stretching band at ~ 1050 cm⁻¹, are present also when CH₃OH is adsorbed on pure MgO samples (spectra not reported for sake of brevity).
2. After a thermal treatment at 523 K in methanol a new band at $\nu \cong 3215$ cm⁻¹ develops, accompanied by the disappearance of the intense absorptions in the $\nu \cong 3600\text{--}3200$ cm⁻¹ range. This band, already observed on other systems [53], could be assigned to the $\nu(\text{OH})$ mode of intermediate species probably adsorbed on palladium particles. The broad character of this band implies that the involved hydroxyl group is perturbed by a hydrogen-bonding interaction with neighboring surface oxygen ions (of the MgO matrix); on the basis of data of Fig. 2, a more detailed assignment is not possible.
3. After treatment at 523 K, narrow bands at $\nu \cong 2945\text{--}2925$, 2832–2818, and 1093 cm⁻¹ are assigned to the asymmetric and symmetric CH₃ stretching modes and to the $\nu(\text{CO})$ of methoxy species. As these bands are

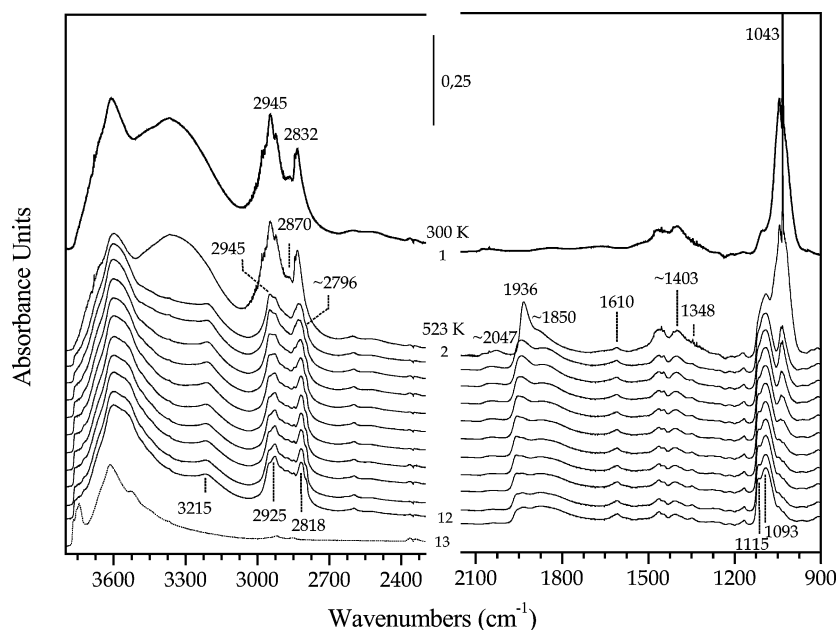


Fig. 2. FTIR spectra of CH_3OH adsorbed on $\text{PdMgO}(\text{Cl})$ outgassed and reduced at 623 K. Curve 1 shows the spectrum of CH_3OH dosed at 300 K ($p = 2.66$ kPa); curve 2 shows the spectrum after thermal treatment in CH_3OH at 523 K; curve 12 shows the spectrum after thermal treatment in CH_3OH at 523 K and at $\theta(\text{CH}_3\text{OH}) \rightarrow 0$; curve 13 shows the spectrum before CH_3OH adsorption.

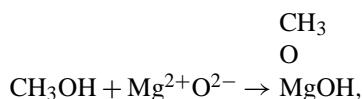
present with similar intensity, when CH_3OH is dosed at 523 K on pristine MgO , it is concluded that these species are adsorbed on the MgO matrix.

- Formation of intense and complex bands in the $\nu \cong 2100\text{--}1700$ cm^{-1} range are due to the stretching mode of carbonyl species adsorbed on Pd particles; the presence of these bands proves unambiguously that CH_3OH decomposes at 523 K on Pd particles.
- Broad bands in the $\nu \cong 1600\text{--}1300$ cm^{-1} range can be assigned to formate intermediate species (vide infra).

It is noteworthy that the absorptions, at $\nu \cong 2076$ and 1992 cm^{-1} , assigned before to linear and bridge-bonded CO species on $\text{CO}/\text{PdMgO}(\text{Cl})$ systems, are now shifted to lower frequency values ($\nu \cong 2047$ and 1936 cm^{-1} , respectively). In addition the features of CO adsorbed on threefold hollow sites are absent: this means that the last sites are probably partially covered by intermediates, arising from methanol decomposition.

From these observations, it follows that:

- Adsorption of CH_3OH is accompanied by formation of hydroxyl groups and methoxy species (either isolated and hydrogen bonded). Their frequency is similar to those obtained on pure MgO and, hence, this behavior is interpreted in terms of the reaction:



which is mainly occurring on the matrix. As MgO is unreactive in methanol decomposition, these species,

taken alone, cannot be considered as intermediates of methanol decomposition in the absence of Pd^0 .

Minor features are present at 3215 cm^{-1} and at 1610 cm^{-1} . The interpretation of these spectroscopic features is not straightforward. Most likely, the band at 3215 cm^{-1} is the $\nu(\text{OH})$ of a hydroxyl group perturbed by hydrogen bonding. We shall return to this point in the following.

- At 523 K the $\text{CH}_3\text{OH} \leftrightarrow \text{CO} + 2\text{H}_2$ reaction is occurring on Pd particles, as indicated by the formation of Pd carbonyls intermediates. This result is remarkable because it demonstrates that the same Pd carbonyl intermediates can be created either by dosing purely CO or by starting from CH_3OH .

On the basis of these data we cannot advance any hypothesis on the decomposition mechanism on Pd particles.

Similar experiments have been performed on the Pd/MgO system (Fig. 3). Upon close inspection of the FTIR spectra of CH_3OH , dosed on Pd/MgO at 300 K and then activated at 523 K (Fig. 3), the following can be observed:

- Broad and intense bands appear in the spectrum of CH_3OH ($p = 2.66$ kPa) in the $\nu = 3600\text{--}3200$ cm^{-1} range, which are assigned to hydrogen-bonded adsorbed CH_3OH on the MgO matrix. Simultaneously, the characteristic C–O stretching band at ~ 1050 cm^{-1} due to physisorbed methanol appears. These bands are reversible upon evacuation.
- Narrow bands develop at $\nu = 2935\text{--}2920$ and $2824\text{--}2805$ cm^{-1} , which are assigned to the asymmetric and symmetric CH_3 stretching modes of methoxy species. Both molecular methanol and chemisorbed methoxy

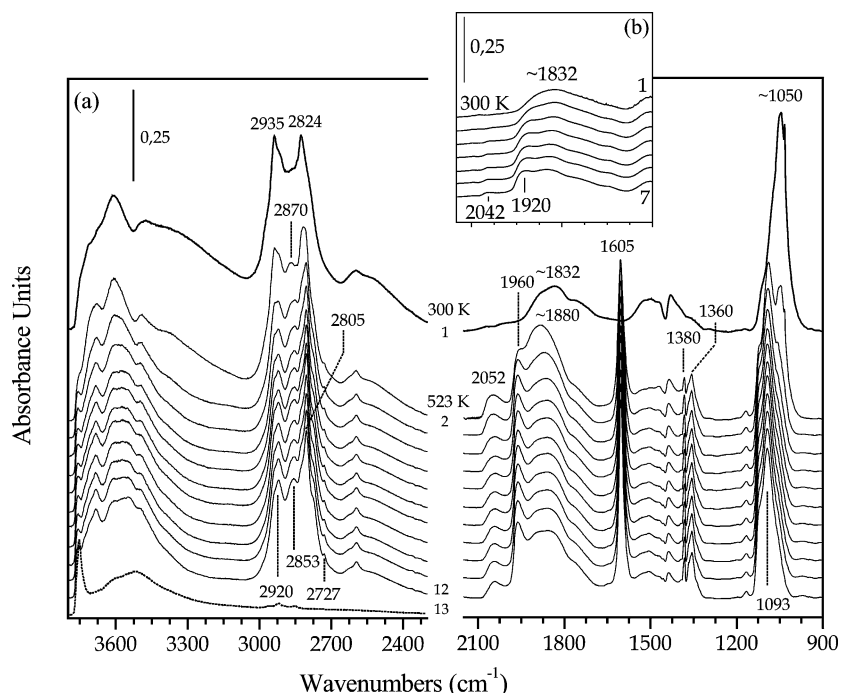
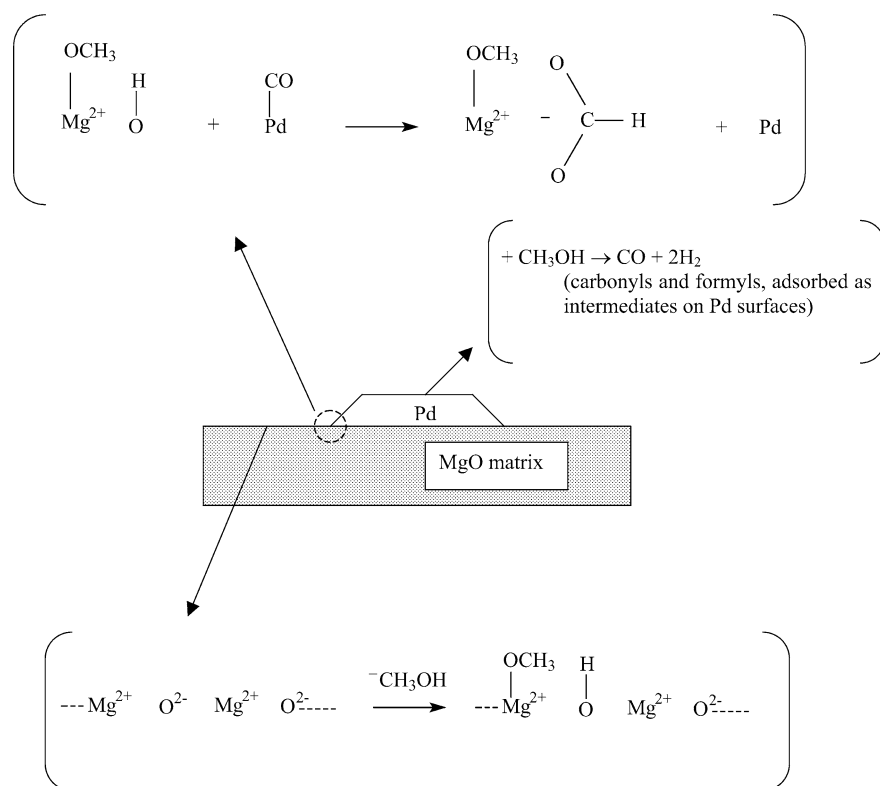


Fig. 3. FTIR spectra of CH_3OH adsorbed on Pd/MgO outgassed and reduced at 623 K. (a) Curve 1 shows the spectrum of CH_3OH dosed at 300 K ($p = 2.66$ kPa); curve 2 shows the spectrum after thermal treatment in CH_3OH at 523 K; curve 12 shows the spectrum after thermal treatment in CH_3OH at 523 K and at $\theta(\text{CH}_3\text{OH}) \rightarrow 0$; curve 13 shows the spectrum before CH_3OH adsorption. (b) FTIR spectra in the CO stretching region of CH_3OH adsorbed at 300 K on Pd/MgO outgassed and reduced at 623 K (curve 1 shows the spectrum at $p(\text{CH}_3\text{OH}) = 2.66$ kPa; curve 7 shows the spectrum at $p(\text{CH}_3\text{OH}) \cong 2$ Pa).

groups are expected to contribute here. The simultaneous presence of physisorbed and chemisorbed species on the surface is also proved by the C–O stretching absorptions bands. This behavior has already been observed on different supports [2].

3. A broad and complex absorption appears in the 2200–1500 cm^{-1} range (with apparent maximum at 1832 cm^{-1}). This absorption is attributed to CO species adsorbed on Pd particles. The frequency of these bands is influenced by the presence of physisorbed methanol (see inset). The presence of carbonylic species on Pd already present at 300 K indicates that methanol decomposes already at 300 K on the Pd particles of the Pd/MgO system. On this basis we conclude that Pd/MgO is more active than Pd/MgO(Cl) (at room temperature). This effect is plausibly related to the effect of Cl ions on Pd/MgO. In a previous paper of this series [51], we have demonstrated that Cl^- ions, present on the surface (less than 1% by weight, as determined by EDAX analysis), are substituting the most basic O^{2-} surface ions, so leading to a dramatic decrease of the basicity of the matrix. That surface Cl is decreasing the surface basicity is shown by independent experiments carried out on Cl-doped MgO, where it has demonstrated that the formation of $\text{C}_n\text{O}_{n+1}^{2-}$ anions by interaction of CO with strongly basic O^{2-} ions is heavily suppressed [54, and references therein]. Similar results have been obtained by substituting basic O^{2-} ions with the less basic S^{2-} [54].

4. Upon increasing the temperature to 523 K, the spectroscopic signatures of physically adsorbed CH_3OH decline, while those characteristic of chemically adsorbed species on MgO matrix and on Pd become dominant. In particular an intense and sharp band at 1605 cm^{-1} associated with a couple of bands at 1440–1360 cm^{-1} is observed, which is assigned to the OCO asymmetric and symmetric stretching modes of an intermediate formate species adsorbed on $\text{Mg}^{2+}\text{O}^{2-}$ pairs, absent on the Pd/MgO(Cl) system [55]); one additional weak band at 2727 cm^{-1} is also observable, which could be assigned to a combination of the C–H bending and of the OCO symmetric stretching frequency of the formate species [56] or less likely to a C–H stretching mode of a HCO formyl group [57]. The second hypothesis is highly tentative because the typical C=O band, appearing as a shoulder at $\nu \cong 1700$ cm^{-1} and associated with the HCO formyl group is very weak.
5. The typical bands in the $\nu = 2150$ –1700 cm^{-1} range are due to the stretching modes of carbonyl species adsorbed on Pd particles. In particular, the absorptions, at $\nu \cong 2060$ and 1970 cm^{-1} , already observed on CO/Pd/MgO systems and assigned to linear and bridge-bonded species, are now shifted to lower frequency values ($\nu = 2052$ and 1960 cm^{-1} , respectively). The band, previously observed on this system at $\nu = 1920$ cm^{-1} , is now absent. On the contrary a new band at $\nu \cong 1880$ cm^{-1} appears, which could be associated with a CO species on threefold hollow sites.



Scheme 1.

Table 1
Surface species resulting from the reaction of CH₃OH adsorbed on Pd/MgO

Frequency (cm ⁻¹)	Type of species	Type of vibration
3600–3200	Hydroxyl group	Hydrogen bonded
~ 1050	Carbonyl group	C–O stretching
2935–2920	Methoxy group	Asymmetric CH ₃ stretching
2824–2805	Methoxy group	Symmetric CH ₃ stretching
2870	Formate-type group	C–H stretching
1380	Formate-type group	C–H bending
1605	Formate-type group	Asymmetric OCO stretch
1360	Formate-type group	Symmetric OCO stretch
2727	Formate combination or formyl	C–H stretching
2150–1700	Carbonyl	CO stretching of Pd ⁰ (CO) species

All these bands behave as irreversible species, i.e., the intensity cannot be decreased by removing the gas phase at 300 K.

We can summarize the previous assignments in Table 1.

In conclusion, on the basis of the FTIR spectra of CH₃OH adsorbed on Pd/MgO surfaces, a plausible mechanism for the methanol decomposition can be hypothesized. At first, it is relevant to note that all the species noted in the table coexist on the surface, so this reaction leads to the simultaneous formation of carbonyl species on Pd particles (at room temperature) and methoxy species mainly adsorbed on Mg²⁺ sites.

As the formate species are formed only at 523 K, they do not play a role in the methanol decomposition on Pd

particles. Here, we may raise the question, Why we do observe formate species only on the Pd/MgO system, but not on Pd/MgO(Cl) and on Pd/Al₂O₃? The answer must be related to the surface basicity of the matrix, which is decreased on the Pd/MgO(Cl) and Pd(Al₂O₃) systems. A mechanism which can explain the role of basicity in the formation of formate species is reported in Scheme 1.

As suggested by an anonymous referee the presence of formates can be related to the superior activity of the Pd/MgO system. The basic idea is that CO adsorbed on pure Pd surfaces blocks the dehydrogenation reaction, as recently highlighted, e.g., by Bowker et al. [59]. Thus the main role of the basic support (together with MeOH) appears to be the removal of CO from Pd, via the formation of formate groups adsorbed on the matrix. Vice versa the synthesis of MeOH from CO/H₂ could be promoted by the simultaneous action of MeOH and CO on the support leading to formate, etc. This hypothesis is strengthened by the observation that exposure of the pristine MgO support to MeOH and CO does not lead to complete methanol decomposition. Analogous reaction pathways can be hypothesized for formyl groups, which can be transformed into formate species by interaction with basic O²⁻ ions of the matrix. In other words the basic matrix allows the capture of products originally formed on Pd. This reaction does not occur when CO is dosed on pure MgO. Hence it requires the participation of Pd particles. It is quite conceivable that the reactive CO is really a PdCO species located at the border of the Pd particles.

The cooperation between the Pd particles and the basic matrix in the stabilization and enrichment of intermediates with a formate-type structure could play a role in explaining the superior activity of Pd/MgO in the synthesis of methanol from CO + H₂ (vide infra).

3.2.1. FTIR spectra of adsorbed CO/H₂ mixture (1/2)

Having established that Pd/MgO is more reactive in methanol decomposition we have studied the CH₃OH synthesis on the same sample.

In Fig. 4 FTIR spectra are reported, which were obtained when a mixture of CO (6.65 kPa) and H₂ (13.3 kPa) were dosed on the Pd/MgO sample. The temperature dependence of the reaction process was investigated in the range from 423 to 473 K. The reaction of the CO/H₂ mixture on Pd/MgO at 423 K (curve 2, reaction time: 15 min) and at 473 K (curve 3) gives rise to carbonyls species adsorbed on Pd particles (bands at 2065, 1968, and 1870 cm⁻¹). Hydrogenation of these carbonyl species first yields an intermediate formyl species (band at 2727 cm⁻¹) and, later, formate species adsorbed on different sites as the carbonyl species (bands at 2850, 1380, 1605, and 1360 cm⁻¹). These experiments demonstrate that the same carbonyl and formate species can be formed either by decomposition of methanol or by CO–H₂ reaction.

A similar mechanism of methanol synthesis has been proposed on alkali/MgO-doped silica-supported Pd catalysts, where a good correlation between the concentration of the detected formyl species and the activity of the catalyst, dependent on the percentage of the MgO, was found [58].

3.2.2. IRAS spectra of CH₃OH decomposition on Pd model catalysts

Here, we focus on the temperature dependence of methanol decomposition and on the interpretation of the IR spectra of adsorbed CO, formed as a product of methanol dehydrogenation. For more information on the mechanism of methanol adsorption and decomposition [60] and on the kinetics of dehydrogenation [61] we refer to studies published recently.

IR spectra recorded during methanol adsorption on the Pd/Al₂O₃ model catalyst (type I) at a sample temperature of 100 K are displayed in Figs. 5(a–d).

We observe bands in the OH stretching (~3300 cm⁻¹), CH stretching (2985, 2956, and 2832 cm⁻¹), CH deformation (~1460 cm⁻¹), CH rocking (~1120 cm⁻¹), and CO stretching (~1030 cm⁻¹) frequency region, indicating preferential molecular adsorption of CH₃OH. No CO is observed at this temperature, showing that no dehydrogenation occurs under these conditions. A detailed discussion of the assignments and intensity effects of the various bands is given elsewhere [60]. For the present discussion, we only note that in the CO stretching frequency region we observe the successive appearance of two bands at approximately 1005–1020 and 1040 cm⁻¹ (followed by multiple signals in the region of 1025 to 1050 cm⁻¹, indicating multilayer adsorption). These two bands have been assigned to methanol adsorbed on the Pd particles and on the alumina film, respectively, with the sequential population, indicating preferential adsorption on the particles [60].

IR spectra, shown in Figs. 5e–5h, have been acquired during methanol exposure at successively higher temperature. At 100 K, multilayers of molecular methanol can be accumulated, which desorb in a temperature range between

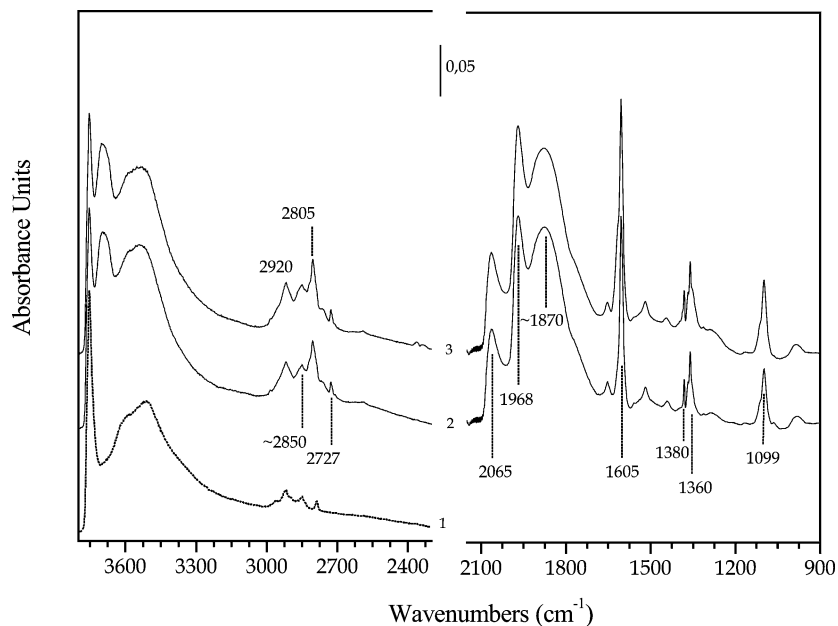


Fig. 4. FTIR spectra of CO/H₂ mixture (1/2) adsorbed on Pd/MgO outgassed and reduced at 623 K: exposure at 423 K for 15 min (curve 2) and at 473 K for 15 min (curve 3). Curve 1 reports the spectrum before CO/H₂ mixture adsorption.

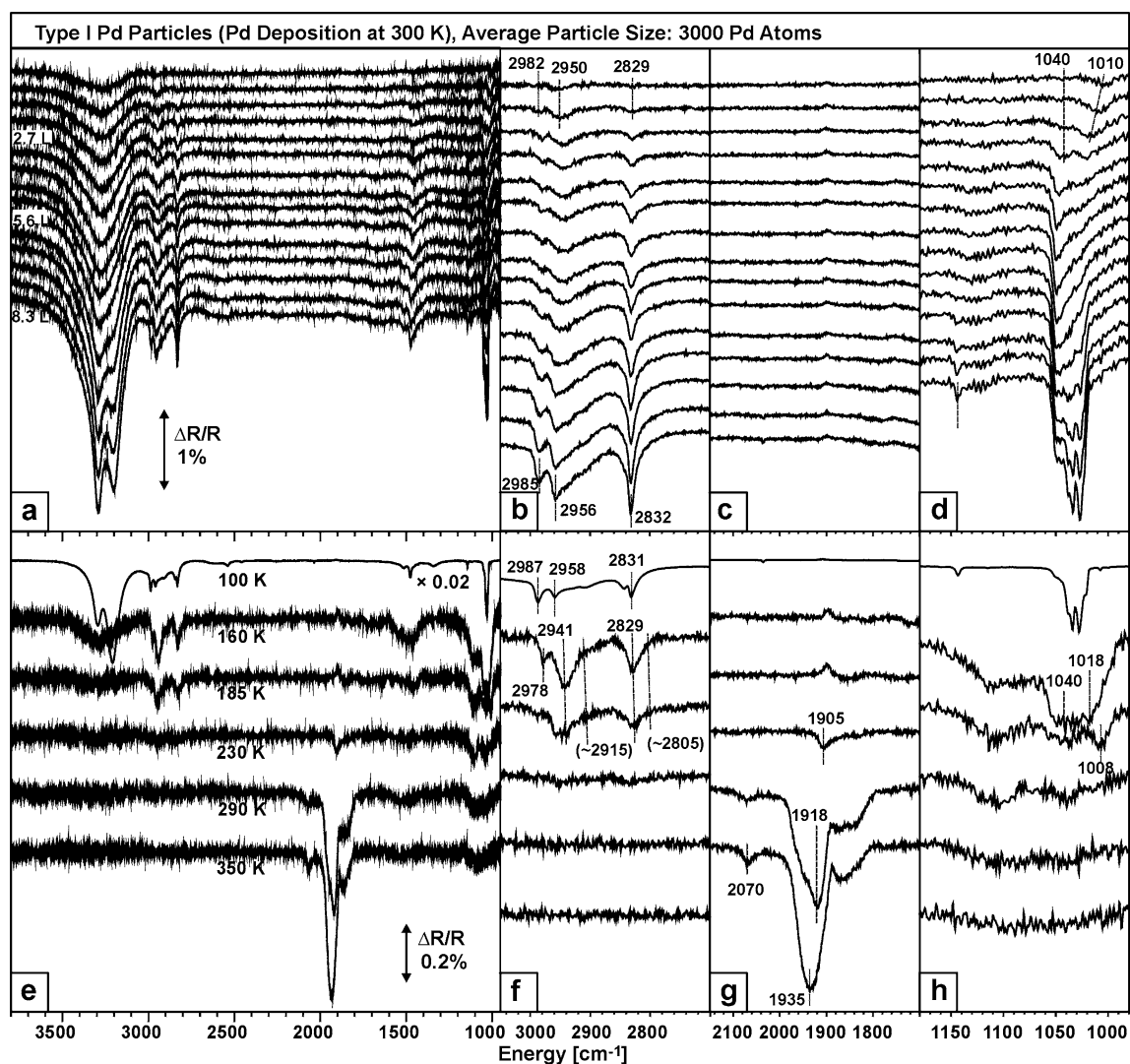


Fig. 5. IR reflection absorption spectra recorded during methanol adsorption at 100 K (a–d) and during methanol decomposition at various temperatures (e–h) on a Pd model catalyst of type I. The spectra e–f were recorded during exposure to a molecular beam of methanol (in Ar as a carrier gas, see text for details).

140 and 150 K. At 160 K, molecular methanol adsorbs on both the Pd particles and the alumina film, as indicated by the presence of both characteristic C–O stretching frequency bands. As it has been shown by isotope exchange experiments in a previous study, indications for the formation of methoxy species are observed in a temperature range between 160 and 200 K (typically indicated by shoulders in the CH stretching frequency range around 2805 and 2915 cm^{-1} ; see [60]). At 185 K, CO desorbs from the alumina support and remains present on the Pd particles only (band at 1008 cm^{-1}). No formation of CO is found up to 185 K (note that the weak feature around 1900 cm^{-1} at temperatures between 100 and 185 K is due to a small CO contamination formed during preparation, but not due to methanol dehydrogenation. Broad features in the frequency range around 1500 cm^{-1} are caused by the limited baseline stability of variable temperature experiments).

At temperatures of 200 K and above CO is formed as a product of methanol dehydrogenation (see Fig. 5g). The

corresponding absorption feature around 1900 cm^{-1} indicates that the CO species produced are adsorbed in hollow sites (see also [60]), presumably on the particle facets. It is noteworthy that no intermediates other than methoxy are observed, indicating that all following dehydrogenation steps are fast, so that intermediates other than methoxy cannot be stabilized on the model catalyst. With increasing reaction temperature the CO coverage on the particles increases: at 290 K, we observe a dominating absorption band at 1918 cm^{-1} and a broad feature around 1860 cm^{-1} . The absence of the bands in the range between 1950 and 2000 cm^{-1} (disregarding a weak shoulder in this region) indicates the absence of bridge-bonded CO at the particle edges. This observation can be explained by an occupation and blocking of the particle facet sites by CO, leading to an inhibition of methanol dehydrogenation and resulting in the reaction to stop before the edge sites are fully occupied. Note that carbon formation as a possible alternative explanation for the missing bridge-bonded CO can be excluded, as

no significant enhancement in the on-top CO region is observed (see discussion in part I).

If we proceed to even higher temperatures (see Fig. 5g, 350 K), CO desorption occurs and allows continuous dehydrogenation during exposure to the methanol beam (see [61] for details on the kinetics). Correspondingly, the CO spectra correspond to a steady-state situation under reaction conditions. At this temperature, bridge-bonded sites at the particle edges are found to be partially occupied only. Interestingly, the slightly enhanced CO peak in the on top-region (approx 2070 cm^{-1}) may indicate a beginning of carbon contamination due to methanol C–O bond scission [12].

4. Conclusions

On polycrystalline Pd/MgO(Cl) and Pd/MgO systems methanol decomposition leads to the simultaneous formation of carbonyl species on Pd particles (at room temperature) and methoxy species mainly adsorbed on Mg^{2+} sites. The fact that the formate species are formed only on the Pd/MgO at 523 K can be explained by the basic character of the MgO matrix. The basic groups (OH^-) of MgO, in the immediate vicinity of Pd particles or at their border, are able to capture species from Pd^0 particles. Among these species can be, e.g., CO, or formyl groups (HCO) formed initially on the Pd by dehydrogenation of CH_3OH .

Thus, the basic matrix may help to identify intermediates originally formed on Pd particles. Specifically in the case of formyl groups these cannot be directly observed on Pd^0 . In conclusion the cooperation between the Pd particles and the basic matrix in the stabilization and enrichment of intermediates with formate-type structure could play a role in explaining the superior activity of Pd/MgO in the synthesis of methanol from $\text{CO} + \text{H}_2$ (vide infra).

The experiments on Pd/MgO and Pd/MgO(Cl) do not give direct evidence about the reactions occurring on bare Pd surfaces. This problem is better tackled by the IRAS studies on Pd/ Al_2O_3 model catalysts.

On well-defined single-crystal-based Pd/ Al_2O_3 model catalysts prepared under UHV conditions two methanol decomposition pathways are observed, i.e., dehydrogenation and C–O bond scission. Both pathways exhibit a characteristic temperature dependence and are affected in a different manner by carbon and CO coadsorbates.

At low temperatures (around 200 K) no intermediates other than methoxy are observed, indicating that all dehydrogenation steps are fast, so that intermediates other than methoxy cannot be stabilized on the model catalyst. Complete dehydrogenation occurs at temperatures of 200 K and above and strongly depends on the CO coverage of the system. At higher temperatures (350 K), the relative occupation of bridge bonded and on top sites in the vicinity of particle edges and defects is indicative of the onset of methanol C–O bond scission and the resulting formation of carbon contaminations.

In conclusion, supported model catalyst with a reduced level of complexity and well-defined surfaces allow us to assign adsorbed species to specific sites on the particles and, as a result, to advance plausible reaction mechanisms. On the other hand, the study of the dispersed Pd/MgO system reveals specific cooperative effects between Pd and the support, which are not accessible under the experimental conditions of the model studies. The support captures fragments formed on Pd surfaces during CH_3OH decomposition (or $\text{CO} + \text{H}_2$ reaction), making them observable by vibrational spectroscopy. This type of metal/support cooperative effect may also play a role in methanol synthesis.

Acknowledgments

This project has been supported by Italian MIUR (COFIN 1998 and 2000, Area 03), by the Deutsche Forschungsgemeinschaft (SPP 1091) and the Volkswagen Foundation (Program of Partnerships). We thank K.M. Neyman and C.S. Gopinath for helpful discussions.

References

- [1] B.C. Bond, Surf. Sci. 156 (1985) 966.
- [2] S. Schauer mann, J. Hoffmann, V. Johánek, J. Hartmann, J. Libuda, H.-J. Freund, Angew. Chem. Int. Ed. 41 (2002) 2532.
- [3] G. Rupprechter, K. Hayek, H. Hofmeister, J. Catal. 173 (1998) 409.
- [4] J.L. Carter, J.A. Cusumano, J.H. Sinfelt, J. Phys. Chem. 70 (1966) 2257.
- [5] M. Boudart, A.W. Aldag, L.D. Ptak, J.E. Benson, J. Catal. 11 (1968) 35.
- [6] T.A. Dorling, B.W. Lynch, R.L. Moss, J. Catal. 20 (1971) 190.
- [7] P.H. Otero-Schipper, P.A. Wachter, J.B. Butt, R.L. Burwell, J.B. Cohen, J. Catal. 53 (1978) 414.
- [8] I.Ko. Edmond, S. Winston, C. Woo, J. Chem. Soc. Chem. Commun. (1982) 740.
- [9] Y. Saitoh, S. Ohtsu, Y. Makie, T. Okada, K. Satoh, N. Tsuruta, Y. Terunuma, Bull. Chem. Soc. Jpn. 63 (1990) 108–115.
- [10] G. Rupprechter, G. Seeber, H. Goller, K. Hayek, J. Catal. 186 (1999) 201–213.
- [11] K. Hayek, M. Fuchs, B. Klötzer, W. Reichl, G. Rupprechter, Top. Catal. 13 (2000) 55.
- [12] M.L. Poutsma, L.F. Eleck, P.A. Ibarbia, A.P. Risch, J.A. Rabo, J. Catal. 52 (1978) 156.
- [13] J.P. Hindermann, G.J. Hutchings, A. Kiennemann, Catal. Rev.-Sci. Eng. 35 (1993) 1.
- [14] M.L. Cubeiro, J.L.G. Fierro, J. Catal. 179 (1998) 150.
- [15] E.M. Cordi, J.L. Falconier, J. Catal. 162 (1996) 104.
- [16] J. Hoffmann, S. Schauer mann, V. Johánek, J. Hartmann, J. Libuda, J. Catal. 213 (2003) 176.
- [17] V. Johánek, S. Schauer mann, M. Laurin, J. Libuda, H.J. Freund, Angew. Chem. Int. Ed. 42 (2003) 3035.
- [18] Y. Matsumura, M. Okumura, Y. Usami, K. Kagawa, H. Yamashita, M. Anpo, M. Haruta, Catal. Lett. 44 (1997) 189.
- [19] Y. Usami, K. Kagawa, M. Kawazoe, Y. Matsumura, H. Sakurai, M. Haruta, Appl. Catal. A 171 (1998) 123.
- [20] N. Iwasa, O. Yamamoto, T. Akazawa, S. Ohshima, N. Takezawa, J. Chem. Soc., Chem. Commun. (1991) 1322.
- [21] Y. Saitoh, S. Ohtsu, Y. Makie, T. Okada, K. Satoh, N. Tsuruta, Y. Terunuma, Bull. Chem. Soc. Jpn. 63 (1990) 108.

- [22] D.T. Wickahm, B.W. Logsdon, S.W. Cowley, *J. Catal.* 128 (1991) 198.
- [23] J.M. Driessen, E.K. Poels, J.P. Hindermann, V. Ponc, *J. Catal.* 82 (1983) 26–34.
- [24] W.J. Shen, M. Okumura, Y. Matsumura, M. Haruta, *Appl. Catal. A* 213 (2001) 225.
- [25] G.C. Cabilla, A.L. Bonivardi, M.A. Baltanas, *Catal. Lett.* 55 (1998) 147.
- [26] V.L. Kirillov, Y.A. Ryndin, *React. Kinet. Catal. Lett.* 59 (1996) 351.
- [27] A. Gotti, R. Prins, *J. Catal.* 175 (1998) 302.
- [28] V.P. Zhdanov, B. Kasemo, *Surf. Sci. Rep.* 39 (2000) 25.
- [29] C. Henry, *Surf. Sci. Rep.* 31 (1998) 231.
- [30] R.P. Holroyd, M. Bowker, *Surf. Sci.* 377–379 (1997) 786.
- [31] J.-J. Chen, Z.-C. Jiang, Y. Zhou, B.R. Chakraborty, N. Winograd, *Surf. Sci.* 328 (1995) 248.
- [32] M. Rebholz, V. Matolin, R. Prins, N. Kruse, *Surf. Sci.* 251 (1991) 1117.
- [33] J.L. Davis, M.A. Barteau, *Surf. Sci.* 235 (1990) 235.
- [34] X. Guo, L. Hanley, J.T. Yates Jr., *J. Am. Chem. Soc.* 111 (1989) 3155.
- [35] R.J. Levis, Z.C. Jiang, N. Winograd, *J. Am. Chem. Soc.* 111 (1989) 4605.
- [36] A.K. Bhattacharya, M.A. Chesters, M.E. Pemble, N. Sheppard, *Surf. Sci.* 206 (1988) L845.
- [37] K. Christmann, J.E. Demuth, *J. Chem. Phys.* 76 (1982) 6318.
- [38] K. Christmann, J.E. Demuth, *J. Chem. Phys.* 76 (1982) 6308.
- [39] S.M. Francis, J. Corneille, D.W. Goodman, M. Bowker, *Surf. Sci.* 364 (1996) 30.
- [40] M. Mavrikakis, M.A. Barteau, *J. Mol. Catal. A* 131 (1998) 135.
- [41] V.P. Zhdanov, B. Kasemo, *Surf. Sci. Rep.* 39 (2000) 25.
- [42] C.R. Henry, *Surf. Sci. Rep.* 31 (1998) 231.
- [43] M. Bäumer, H.-J. Freund, *Prog. Surf. Sci.* 61 (1999) 127; H. Unterhalt, G. Rupprechter, H.-J. Freund, *J. Phys. Chem. B* 106 (2002) 356.
- [44] C.T. Campbell, A.W. Grant, D.E. Starr, S.C. Parker, V.A. Bondzie, *Top. Catal.* 14 (2001) 43.
- [45] T.P. St. Clair, D.W. Goodman, *Top. Catal.* 13 (2000) 5.
- [46] R.M. Jaeger, H. Kuhlenbeck, H.-J. Freund, M. Wuttig, W. Hoffmann, R. Franchy, H. Ibach, *Surf. Sci.* 259 (1999) 235.
- [47] J. Libuda, F. Winkelmann, M. Bäumer, H.-J. Freund, T. Bertrams, H. Neddermeyer, K. Müller, *Surf. Sci.* 318 (1994) 61.
- [48] J. Libuda, H.-J. Freund, *J. Phys. Chem. B* 106 (2002) 4901.
- [49] J. Libuda, H.-J. Freund, *J. Phys. Chem. B* 106 (2002) 4901.
- [50] S. Shaikhutdinov, M. Heemeier, M. Bäumer, T. Lear, D. Lennon, R.J. Oldman, S.D. Jackson, H.-J. Freund, *J. Catal.* 200 (2001) 330.
- [51] S. Bertarione, D. Scarano, A. Zecchina, V. Johánek, J. Hoffmann, S. Schauer mann, M.M. Frank, J. Libuda, G. Rupprechter, H.-J. Freund, *J. Phys. Chem. B* (2004), accepted for publication.
- [52] I. Meusel, J. Hoffmann, J. Hartmann, M. Heemeier, M. Bäumer, J. Libuda, H.-J. Freund, *Catal. Lett.* 71 (2001) 5.
- [53] G.-W. Wang, H. Hattori, *J. Chem. Soc., Faraday Trans. 1* 80 (1984) 1039–1047.
- [54] D. Scarano, S. Bertarione, A. Zecchina, R. Soave, G. Pacchioni, *Phys. Chem. Chem. Phys.* 4 (2002) 366.
- [55] K. Nakamoto, *IR and Raman Spectra of Inorganic and Coordination Compounds*, third ed., Wiley, New York, 1978.
- [56] J.F. Edwards, G.L. Schrader, *J. Catal.* 94 (1985) 175–186.
- [57] D. Loffreda, D. Simon, P. Sautet, *Surf. Sci.* 425 (1999) 68.
- [58] Z. Karpinski, I. Ratajczykowa, W. Palczewska, *Ann. Rep. Progr. Chem. C* 81 (1984) 160.
- [59] M. Bowker, R.P. Holroyd, R.G. Sharpe, J.S. Corneille, S.M. Francis, D.W. Goodman, *Surf. Sci.* 370 (1997) 113; R.P. Holroyd, M. Bowker, *Surf. Sci.* 377–379 (1997) 786.
- [60] S. Schauer mann, J. Hoffmann, V. Johánek, J. Hartmann, J. Libuda, *Phys. Chem. Chem. Phys.* 4 (2002) 3909.
- [61] J. Hoffmann, S. Schauer mann, V. Johánek, J. Hartmann, J. Libuda, *J. Catal.* 213 (2003) 176.